Dose-Response:
An International Journal
January-March 2020:1-10

DOI: 10.1177/1559325820904600
journals.sagepub.com/home/dos
SAGE

Screening for Potential Biomarkers in Peripheral Blood From Miners Exposed to Radon Radiation

Lu Sun[1,2], Yan Pan[1], Xiaochun Wang[3], Gang Gao[1], Lina Wu[1], Chunnan Piao[1], Jianlei Ruan[1], and Jianxiang Liu[1]

Abstract

In this cohort study of 144 miners, 72 miners worked underground (the study group) and 72 miners worked aboveground (the control group). Based on questionnaire data and of radon concentration measurements, the cumulative radon exposure dose was calculated for each miner using the parameters recommended in International Commission on Radiological Protection Publication 137. Hematological parameters such as lymphocyte count (LYM) and neutrophil count (NE) were assessed, cell cycle phases and regulatory proteins were detected by flow cytometry, and microRNA (miRNA) microarray screening and real-time polymerase chain reaction (PCR) were used to detect miRNAs in plasma. The interrelationships between various potential biomarkers were analyzed using bioinformatics and statistical methods. The mean cumulative exposure dose of underground miners and controls was 982 and 48 mSv, respectively. Hematological parameters (such as LYM and NE) were significantly lower in the underground group. Cyclin-dependent kinase (CDK)-2, CDK4, CDK6, CyclinA2, CyclinD1, and CyclinE1 were significantly higher in the underground group. MicroRNA microarray screening showed that 5 miRNAs were downregulated (fold-change >2) in the underground group. The real-time PCR detection results of miR-19a, miR-30e, miR-335, and miR-451a were consistent with the screening results. LYM, NE, CDK2, CDK4, CDK6, Cyclin A2, Cyclin D1, Cyclin E1, miR-19a, miR-30e, miR-335, and miR451a are potential biomarkers of radon radiation damage.

Keywords

radon, miners, biomarkers, lymphocytes

Introduction

Radon is a class I carcinogen according to the International Agency for Research on Cancer. Radon and its progeny, which are decay products of radium, are radioactive and represent the second largest cause of lung cancer after smoking.[1,2] Historically, there has been a high incidence of lung cancer among miners. Epidemiological research has shown that radon and smoking are the causes of the high incidence of lung cancer among miners.[3-5] The association between radon exposure and the relative risk of lung cancer is approximately linear.[6] A proportion of inhaled radon is chemically inert, enters the blood circulation, and acts on the human body.[7] Therefore, with increases in radon exposure, are there any potential biomarkers in peripheral blood that can reflect the corresponding damage changes? Quiescent lymphocytes are human immune cells that are highly differentiated nonproliferating cells. Because of their sensitivity to radiation, mature lymphocytes are vulnerable to radiation damage. Immune cells are responsible for performing immune functions, including immune defense, immune homeostasis, and immune monitoring. In the immune response, lymphocytes are often the most important immune cells and play a central role. Cell cycle disorders are tightly associated with diseases

[1] Key Laboratory of Radiological Protection and Nuclear Emergency, National Institute for Radiological Protection, Chinese Center for Disease Control and Prevention, Beijing, China
[2] Liaoning Center for Disease Control and Prevention, Shenyang, China
[3] The Beijing Prevention and Treatment Hospital of Occupational Disease for the Chemical Industry, Beijing, China

Received 24 October 2019; received revised 28 November 2019; accepted 20 December 2019

Corresponding Author:
Jianxiang Liu, No. 2, Dewai Xinkang Road, Xicheng District, Beijing 100088, China.
Email: liujianxiang@nirp.chinacdc.cn

such as cancer. Cell damage can occur at all stages of the cell cycle, but cells are more sensitive to radiation damage during G_1 DNA replication. Cell cycle regulatory proteins include cyclins and cyclin-dependent kinases (CDKs). CyclinD activates CDK4/CDK6 to initiate the cell cycle in the early G_1 phase; CyclinE activates CDK2 in the late G1 phase; Cyclin A/CDK2 and Cyclin B/CDK1 participate in mitosis.[8,9] Further research on the changes in lymphocytes induced by radon in the blood is crucial.

MicroRNAs (miRNAs) are small noncoding RNAs of 19 to 23 nucleotides in length that are important in the regulation of vital biological processes, such as cell proliferation, cell differentiation, endocrine homeostasis, and apoptosis.[10-12] It is estimated that more than 30% of protein-coding genes are regulated by miRNAs, which degrade messenger RNAs (mRNAs) or block translation by completely or partially binding to their target mRNAs. Currently, miRNAs are used to detect carcinomas, select appropriate treatment options, and evaluate the efficacy of radiotherapy.[13-16] Therefore, the changes in miRNAs caused by radon radiation damage are also worth studying.

Epidemiological studies have explored the etiology of lung cancer based on the outcome event (ie, the development of lung cancer) in human populations. Additionally, cell and animal experiments have been conducted to identify changes in various indicators under radon exposure.[17,18] However, little information is available on the biological changes caused by radon exposure in humans. The aim of this study was to screen for potential biomarkers in peripheral blood from miners exposed to high doses of radon.

Methods and Materials

Study Population

This cohort study involved miners at a tin mine in Yunnan Province in China, and it was approved by the Ethics Committee of the National Institute for Radiological Protection at China Center for Disease Control and Prevention. All the participants signed informed consent forms. The inclusion criteria were as follows: employed as a miner, male, at least 1 year since first employment, and no acute infectious diseases, malignant tumors, or serious family history of genetic diseases. According to their workplaces, the miners were divided into 2 groups: underground miners and aboveground miners (controls).

Questionnaire

Using a self-designed questionnaire, trained local investigators conducted face-to-face surveys of the miners, which involved collecting data on general information, employment, living habits, health status, and knowledge of radon. The questionnaires were self-administered after the survey.

Radon Gas Concentration Measurement

LIH detectors (National Institute for Radiological Protection, Chinese Center for Disease Control and Prevention, China) were used for the radon gas concentration measurement. The detectors were calibrated in a standard radon room at the University of South China. The calibration factor was 4.8 tracks·cm^{-2}·(kBq·m^{-3}·h)$^{-1}$, and the solid track detector material CR-39 (Fukuvi Chemical Industry Co, Ltd, Japan) was used. The detectors were placed where workers were concentrated at relatively fixed positions near walls. After recycling, the CR-39 samples were etched in 6.25 mol/L^1 NaOH solution at 80°C for 8 hours. A microscope (CARL ZEISS, Germany) was used to analyze the results. The radon gas concentration was measured 4 times from November 2017 to July 2019 (for 1 month per season). The overall mean was used to represent the radon gas concentration.

Cumulative Radon Exposure and Radon Exposure Effective Dose

For each miner, a detailed working history (ie, number of hours worked) was derived from the questionnaires. Subsequently, the cumulative exposure to radon and its progeny was calculated in working-level month (WLM) units for each miner based on their place of work (underground or aboveground) according to the following formula, which relates WLM to exposure expressed in terms of the cumulative radon gas activity concentration (in Bq/h/m^3):

$$1\ \mathrm{WLM} = (6.37 \times 10^5/\mathrm{F})\ \mathrm{Bq} \cdot\ \mathrm{h} \cdot\ \mathrm{m}^{-3}$$

where F is the dimensionless radon daughter equilibrium factor, which was 0.4 for aboveground miners and 0.2 for underground miners, according to the 2017 International Commission on Radiological Protection (ICRP) Publication 137.[7]

The effective dose (in mSv) was calculated for each miner, based on the following formula, which indicates the appropriate dose conversion factor, as recommended by ICRP137[7]:

$$10\ \mathrm{mSv/WLM}\ (\mathrm{or}\ 15.7\ \mathrm{nSv/Bq \cdot h \cdot m^{-3}})$$

Blood Sample Collection

Blood samples were collected using tubes containing EDTA anticoagulant. Some of each whole blood sample was used to assess hematological parameters (described below). The remainder was centrifuged to separate the plasma which was stored at −80°C, the cell pellet, which was used to extract lymphocytes. Lymphocytes were extracted using lymphocyte separation medium (GE Healthcare, Marlborough) according to the manufacturer's instructions.

Hematological Parameters

Lymphocyte count (LYM), neutrophil count (NE), white blood cell count (WBC), and platelet count (PLT) in the whole blood were detected using a K-21 automated hematology analyzer (Sysmex, Japan).

Cell Cycle Phase Detection

Lymphocytes were fixed with 70% ice-ethanol and deposited overnight in a refrigerator at 4°C. After washing and centrifugation, the cells were resuspended in 500 mL FxCycle PI/RNAse dye solution and then filtered using a nylon mesh and incubated at room temperature without light for 30 minutes. The cell cycle phases were detected using a FACS-Aria Flow Cytometer (BD Biosciences, United States).

The Cycle Regulatory Proteins Detection

Lymphocytes were fixed with 4% polyformaldehyde solution (Solarbio Company, Beijing, China). After washing and centrifugation, a membrane-breaking fixative solution (BD Biosciences) was used according to the manufacturer's instructions. Thereafter, antibodies against CDK2, CDK4 (CST, Danvers, MA), CDK6, Cyclin A2, Cyclin D1, and Cyclin E1 (Abcam, Cambridge, UK) were added to the sample solution, which was incubated without light for 30 minutes and then assessed by flow cytometry.

RNA Isolation

Total RNA was isolated from the plasma samples using a miRNeasy Serum/Plasma Kit (QIAGEN GmbH, Germany) according to the manufacturer's protocol. For protein denaturation, 200 μL plasma was treated with 1 mL QIAzol (QIAGEN GmbH). Synthetic-cel-miR-39 was spiked to each sample as a means of normalization. After adding 200 μL chloroform, the samples were centrifuged at 12 000 × g for 15 minutes at 4°C. Thereafter, 600 μL of the upper aqueous phase was carefully extracted, treated with 900 μL 100% ethanol, and used in an RNeasy MinElute spin column for RNA extraction. After phenol and other contaminants were washed away, the RNA was then eluted in 30 μL RNase-free water. RNA quality and concentration were assessed using a Nanodrop 2000 spectrophotometer (Thermo Scientific, United States).

GeneChip MiRNA 4.0 Array Screening

A GeneChip miRNA 4.0 Array (Affymetrix), which contains all miRNAs in miRbase Release 2.0 (2578 probes for mature human miRNAs), was used to screen the plasma samples for miRNAs. According to statistics on lung cancer in China, the mean age of lung cancer diagnosis has risen rapidly from 40 years old and peaked at 70 years old.[19] Twenty samples were selected from the underground group and divided into 2 subgroups by age, with 10 samples per group. Group C was <40 years old and group Rn was ≥40 years old. The levels of miRNAs were compared between these 2 groups. The total RNAs in each sample were used for labeling and array hybridization and then array scanning was performed. Thereafter, the scanned images were imported into Affymetrix Expression Console software for grid alignment and expression data analysis.

Real-Time Polymerase Chain Reaction MiRNAs Detection

To validate the microarray results, 4 miRNAs (miR-19a, miR-30e, miR-335, and miR-451a) were selected (on the basis of a high fold-change and a high *P* value) for detection using real-time polymerase chain reaction (PCR), and the results were compared between the underground and control groups. Plasma RNA was reverse-transcribed (RT) to complementary DNA (cDNA) using TaqMan MicroRNA Assays (Applied Biosystems, CA), a TaqMan MicroRNA Reverse Transcription Kit (Applied Biosystems, Lithuania), and TaqMan miRNA primers (Applied Biosystems, Pleasanton), according to the manufacturer's protocol with a slight modification. The total volume was 15 μL. First, 3 μL total RNA was added into the 12 μL RT reaction mixture containing 0.2 μL 100 nM deoxyribonucleotide triphosphates (with deoxythymidine triphosphate), 1 μL MultiScribe Reverse Transcriptase (50 U/μL), 1.5 μL 10× reverse transcription buffer, 0.2 μL RNase Inhibitor (20 U/μL), 8.1 μL nuclease-free water, and 1 μL 5RT primer. Each reaction was incubated at 16°C for 30 minutes, 42°C for 30 minutes, and 85°C for 5 minutes in a Veriti 96-Well Thermal Cycler (Applied Biosystems, United States). The cDNA produced was stored at 4°C.

The TaqMan miRNA-specific primers and probes sequences (Applied Biosystems, Pleasanton) were as follows:

Hsa-miR-19a: 5′-UGUGCAAAUCUAUGCAAAACUGA-3′;
Hsa-miR-30e: 5′-UGUAAACAUCCUUGACUGGAAG-3′;
Hsa-miR-335: 5′-UCAAGAGCAAUAACGAAAAAUGU-3′;
Hsa-miR-451a: 5′-AAACCGUUACCAUUACUGAGUU-3′.

Each 20 μL real-time PCR mixture contained 1.33 μL reverse transcription product, 10 μL TaqMan Universal PCR Master MixII[2×] (no uracil-DNA glycosylase; Applied Biosystems), 1 μL TaqMan Small RNA Assay set [20×], and 7.67 μL nuclease-free water. All samples were run in triplicate. Each reaction was incubated at 95°C for 10 minutes, 40 cycles at 95°C for 15 seconds, and 60°C for 1 minute using a Quantstudio 12K Flex Real-Time PCR System (Applied Biosystems, United States). Using the $2^{-\Delta Ct}$ method, the Ct value for each miRNA was normalized to the Ct value for the spike-in synthetic-cel-miR-39 in each sample to eliminate variation produced during the RNA isolation and quantification processes.[20]

Bioinformatics Analysis of MiRNAs

TargetScan, PicTar, miRBase, and miRanda were used for target gene prediction. The relationships between the miRNAs and human diseases were assessed using the Human microRNA Disease Database version 3.0.

Statistical Analysis

Basic characteristics were summarized using proportions for categorical variables, mean ± standard deviation (SD) for normally distributed continuous variables, and median (interquartile range [IQR]) for non-normally distributed continuous variables. Student *t* test and the nonparametric Wilcoxon test were used to assess differences in the study population characteristics and potential biomarkers between the underground and control groups. One-way analysis of variance was used to identify the differences between multiple groups. Multivariate regression analysis was used to analyze the associations with cumulative radon exposure of the relative expression levels of regulatory proteins, age, body mass index (BMI), Smoking Index, age at first exposure, and cumulative radon exposure. The associations between miRNAs and the factors above were analyzed the same way. Correlations between miRNAs and CDKs/Cyclins were evaluated using the Pearson correlation coefficient. All analyses were performed with R version 3.2.2 (R Foundation for Statistical Computing, Vienna, Austria; https://www.r-project.org/) and Prism version 8.0 (GraphPad, San Diego, California; https://www.graphpad.com/). A P value <.05 was considered statistically significant.

Results

Study Population Characteristics

The study population comprised 144 miners from a tin mine in Yunnan Province in China; 72 miners who worked underground were selected as the study group, and 72 miners who worked aboveground were used as the control group. The median age in the underground group was 45.5 years (IQR: 35-51.8), the median BMI was 24 kg/m^2 (IQR: 22.1-26.4), the median age at first radon exposure was 21 years (IQR: 18-25.5), and the median duration of radon exposure was 19.5 years (IQR: 10-31), with no significant differences between the 2 groups ($P > .05$). The median Smoking Index of underground miners was higher than that in the control group, but the difference was not significant. The mean radon gas concentration was higher in the underground group (7441 Bq/m^3) than the aboveground concentration (284 Bq/m^3; $P < .05$). The mean ± SD cumulative radon exposure underground (98 ± 52 WLM) was higher than that aboveground (5 ± 3 WLM; $P < .05$). The mean ± SD effective radon exposure dose underground (982 ± 518 mSv) was higher than that aboveground (48 ± 27 mSv; $P < .05$; Table 1).

Lymphocyte Count and NE Changes Due to Radon Exposure

There were significant reductions in both LYM and NE in the underground group compared to the control group ($P < .05$; Figure 1A). Additionally, in the underground group, both LYM and NE decreased with duration of radon exposure ($P < .05$; Figure 1B). In the nonsmoking and light smoking subgroups, LYM and NE were nonsignificantly lower in the underground group than the control group. In the moderate smoking subgroup, LYM and NE were significantly lower in the underground group than the control group ($P < .05$). In the heavy smoking subgroup, only LYM (not NE) was significantly lower in the underground group than the control group ($P < .05$; Figure 1C).

Significant negative correlations were found between the cumulative radon exposure and LYM ($r = -0.416$; $P < .05$) or NE ($r = -0.360$; $P < .05$) in peripheral venous blood (Figure 1D). The dose–response relationships (best-fit regression lines) between the effective radon dose and LYM or NE in the underground group were as follows: $y_{LYM} = -0.0008x + 2.4261$ ($R^2 = 0.9901$) and $y_{NE} = -0.0013x + 4.2571$ ($R^2 = 0.9362$; Figure 1E). There were no significant between group differences in WBC or PLT (Figure 1F and G).

Comparison of Cell-Cycle Phases and Cell Cycle Regulatory Proteins in Lymphocytes

The median percentage of G_0G_1 lymphocytes in the underground group (99.51%; IQR: 99.21%-99.68%) was significantly greater than that in the control group (99.28%; IQR: 98.97%-99.57%; $P < .01$; Figure 2A). In contrast, the median percentage of S lymphocytes in the underground group (0.26%; IQR: 0.18%-0.46%) was significantly lower than that in the control group (0.42%; IQR: 0.28%-0.65%; $P < .01$; Figure 2A).

The cell cycle regulatory proteins associated with the G_0G_1 and S phases CDK2, CDK4, CDK6, Cyclin A2, Cyclin D1, and Cyclin E1 were detected by flow cytometry. The median relative expression levels were 0.902 (IQR: 0.752-1.537), 1.027 (IQR: 0.916-1.242), 2.743 (IQR: 1.468-3.477), 1.446 (IQR: 0.775-1.681), 3.595 (IQR: 1.332-4.732), and 5.552 (IQR: 3.767-8.884), respectively, in the underground group and 0.731 (IQR: 0.639-0.856), 0.932 (IQR: 0.851-0.989), 1.392 (IQR: 1.271-1.568), 0.715 (IQR: 0.578-1.020), 1.242 (IQR: 1.067-1.445), and 3.512 (IQR: 2.716-4.907), respectively, in the control group. The relative expression levels of these CDKs and cyclins in the underground group were higher than those in the control group ($P < .01$; Figure 2B).

MicroRNA Microarray Screening and Real-Time PCR Verification

Using the GeneChip miRNA 4.0 Array, we screened for 5 downregulated miRNAs (in group Rn compared to group C) with a significant negative fold-change >2 and selected 4. The mean ± SD ages of groups C and Rn were 34 ± 4 and 44 ± 10 years old, respectively. The detailed results are shown in Figure 3A.

Table 1. Characteristics of Underground Miners and Controls.

	Underground		Controls		
Total	72 (N)	100 (%)[a]	72 (N)	100 (%)[a]	*P*
Age					
Median age (IQR) in years	45.5	35-51.8	47	36-52	.463
≤30	9	12.5	8	11.1	
31-40	19	26.4	18	25	
41-50	23	31.9	23	31.9	
51-60	21	29.2	23	31.9	
BMI					
Median BMI (IQR) in kg/m^2	24	22.1-26.4	24.6	21.8-26.9	.872
<18.5	0	0	4	5.6	
18.5-23.9	36	50	28	38.9	
24-27.9	27	37.5	29	40.3	
≥28	9	12.5	11	15.3	
Smoking Index					
Median Smoking Index (IQR) in PYS	13.7	0-20.8	5	0-17.6	.053
0	19	26.4	30	41.7	
0-20	35	48.6	30	41.7	
20-30	15	20.8	7	9.7	
>30	3	4.2	5	6.9	
The first radon exposure age					
Median first exposure age (IQR) in years	21	18-25.5	20	18-23	.102
15-19	24	33.3	31	43.1	
20-24	30	41.7	30	41.7	
≥25	18	25	11	15.3	
Duration of radon exposure					
Median duration of exposure (IQR) in years	19.5	10-31	22.5	13-34	.167
1-10	21	29.2	14	19.4	
11-20	19	26.4	18	25	
21-30	13	18.1	12	16.7	
>30	19	26.4	28	38.9	
Radon gas concentration					
Mean radon gas concentration in Bq/m^3	7441	–	284	–	.000
Accumulative radon exposure					
Median accumulative radon exposure (IQR) in WLM	95	48-149	4	3-7	.000
Mean accumulative radon exposure (SD) in WLM	98	52	5	3	
Effective radon exposure dose					
Median effective exposure dose (IQR) in mSv	946	481-1486	44	24-66	.000
Mean effective radon exposure dose (SD) in mSv	982	518	48	27	

Abbreviations: BMI, body mass index; IQR, interquartile range; PYS, pack-years; SD, standard deviation; WLM, working-level month.
[a]Percentages may not sum to 100 because of rounding.

The 4 miRNAs (miR-19a, miR-30e, miR-335, and miR-451a) were selected for real-time PCR verification. Compared with the control group, all 4 were downregulated in the underground group, although miR-335 ($P = .062$) was not significant at the $P < .5$ level, probably due to the limited number of miners in this study. The detailed results are shown in Figure 3B. Thus, the real-time PCR validation results were consistent with the miRNA screening results.

Potential Biomarkers Related to Cumulative Radon Exposure

Age, BMI, Smoking Index, age at first exposure, cumulative radon exposure, LYM, NE, relative expression level of cell cycle regulatory proteins, and miRNAs were introduced into the multiple linear regression analysis. The results showed that LYM, NE, miR-19a, miR-30e, miR-335, and miR-451a were negatively associated with cumulative radon exposure ($P < .05$), while CDK2, CDK4, CDK6, Cyclin A2, Cyclin D1, and Cyclin E1 were positively associated with cumulative radon exposure ($P < .05$). No associations were found for age, BMI, Smoking Index, or age at first exposure ($P > .05$).

Associations Between CDKs, Cyclins, and MiRNAs

Using the Human microRNA Disease Database version 3.0, it was found that the 4 miRNAs mentioned above (miR-19a, miR-30e, miR-335, and miR-451a) are related to human lung carcinoma. To understand whether the 4 miRNAs have

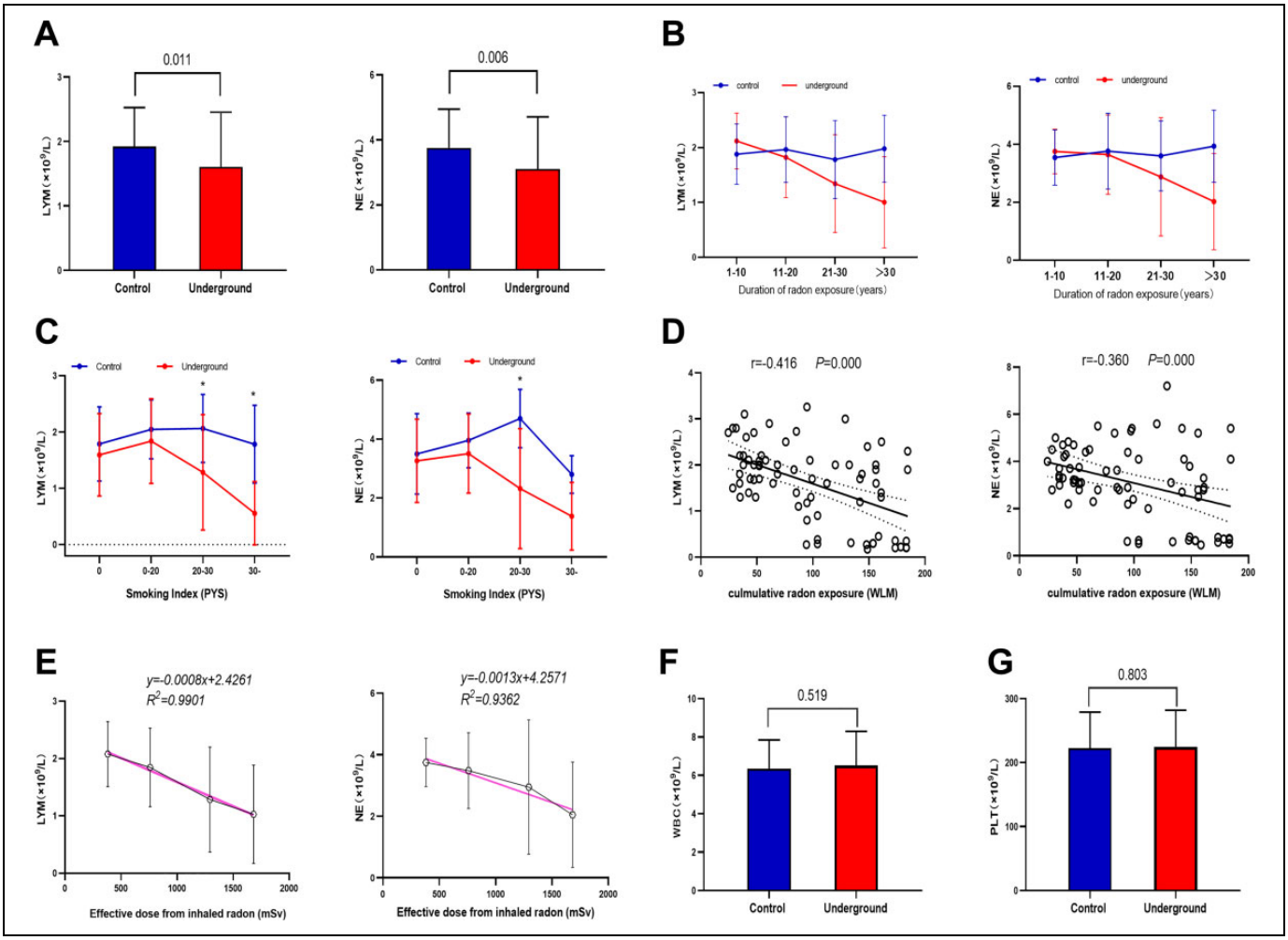

Figure 1. Analysis of hematological parameters. A, Comparison of lymphocyte count (LYM) and neutrophil count (NE) in peripheral venous blood between the 2 groups of miners. B, Changes in LYM and NE with duration of radon exposure. Data represent mean ± standard deviation. C, Changes in LYM and NE across Smoking Index subgroups (0, ≤20, ≤30, and >30; Table 1). D, Significant and negative correlations between cumulative radon exposure and LYM or NE. Pearson correlation coefficients and *P* values were calculated. E, Dose–response relationship between effective dose from inhaled radon and LYM or NE in the underground group. The red regression lines represent the best fitting linear dose–response relationships. Comparison of (F) white blood cell count (WBC) and (G) platelet count (PLT) between the 2 groups of miners, showing no significant differences.

potentially relevant biological effects, we identified their target genes and examined whether these target genes are involved in regulating cell cycle. Target genes, comprising CCNA2 and CCND1 (which encode Cyclin A2 and Cyclin D1, respectively) for miR-19a, CCNE (which encodes Cyclin E1) for miR-30e and CDK2 (which encodes CDK2) for miR-335, were predicted by TargetScan, PicTar, miRBase, and miRanda. No target gene related to the cell cycle was predicted for miR-451a. We then analyzed the correlations between them and found that Cyclin A2 was significantly negatively correlated with miR-19a ($r = -0.272$, $P = .001$), Cyclin D1 was significantly negatively correlated with miR-19a ($r = -0.252$, $P = .002$), Cyclin E1 was significantly negatively correlated with miR-30e ($r = -0.199$, $P = .017$), and CDK2 was significantly negatively correlated with miR-335 ($r = -0.240$, $P = .004$; Figure 4).

Discussion

The detection of biomarkers in peripheral blood is fast, and the blood samples are easily and relatively noninvasively to obtain. In this cohort study, we evaluated the changes of a diverse panel of potential biomarkers in miners' peripheral venous blood after long-term high radon exposure. We found (1) a significant decrease in the LYM in the peripheral venous blood of underground miners exposed to high levels of radon compared to the controls. In the underground group, the G_0/G_1 phase of lymphocytes was prolonged and the S phase was shortened. Regulatory proteins related to the G_0/G_1 and S phases, including CDK2, CDK4, CDK6, Cyclin A2, Cyclin D1, and Cyclin E1, significantly increased in the underground group. MicroRNAs, including miR-19a, miR-30e, and miR-335 (which target Cyclin A2, Cyclin D1, Cyclin E1, and

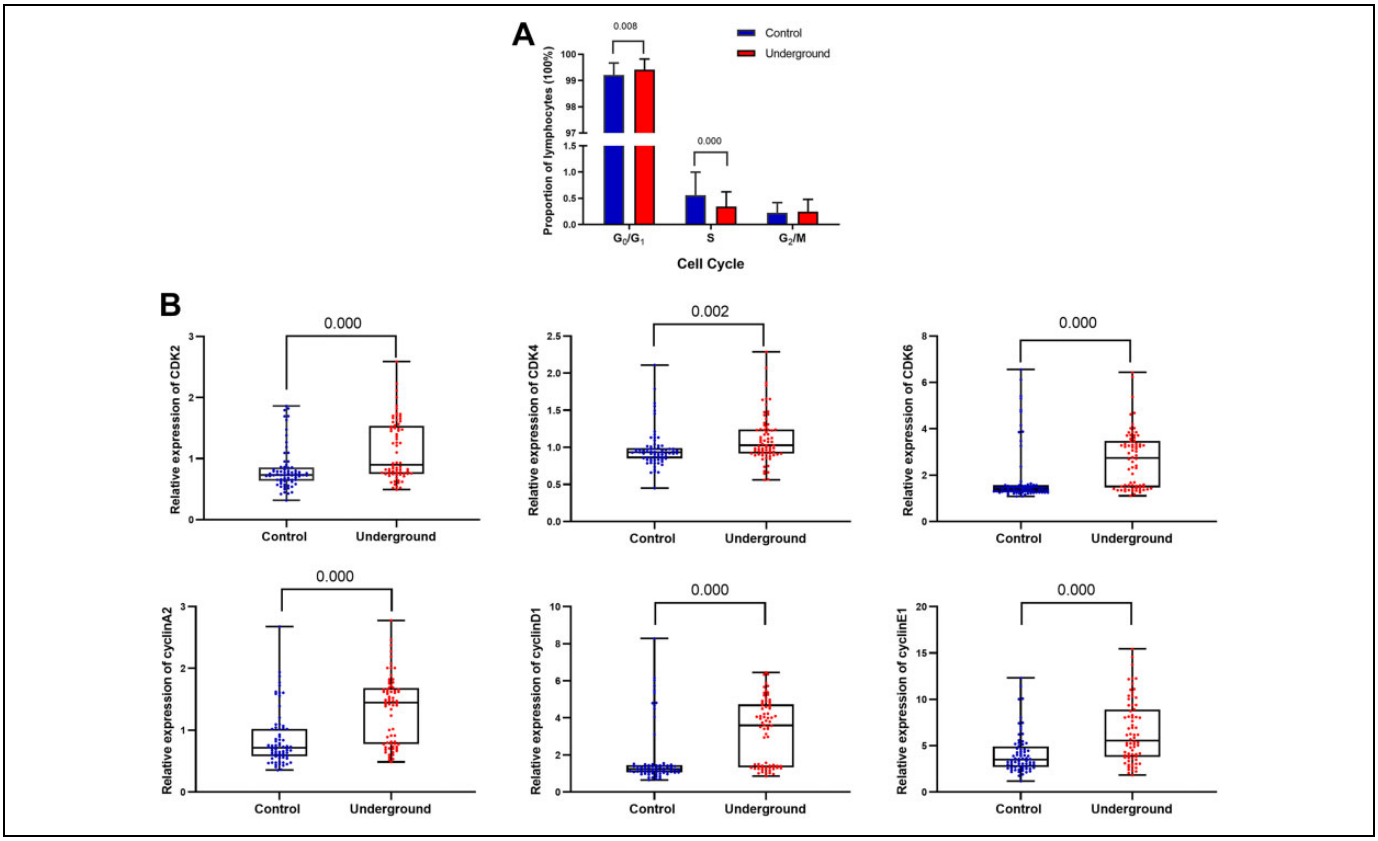

Figure 2. Changes in the cell cycle phases and regulatory proteins in lymphocytes in the underground and control groups. A, Comparison of lymphocyte cell cycle phases between the 2 groups. Data represent median (n = 72 per group). *P* values were calculated using the Wilcoxon test. B, Comparison of relative expression of cell cycle regulatory proteins in the peripheral blood lymphocytes (detected by flow cytometry) between the 2 groups. Data represent median (n = 72 per group). *P* values were calculated using the Wilcoxon test.

CDK2), were significantly downregulated in the underground group compared to the control group; (2) significant associations between potential biomarkers such as LYM, NE, and effective radon dose; and (3) significant negative correlations between certain potential biomarkers, that is, between both Cyclin A2 and Cyclin D1 and miR-19a, between Cyclin E1 and miR-30e, and between CDK2 and miR-335.

The results of the hematological analysis showed that both LYM and NE in the peripheral blood decreased in underground miners, LYM and NE decreased with the duration of radon exposure. These potential biomarkers have a strong linear relationship with the cumulative effective dose of inhaled radon. Lymphocytes are vital immune cells, and their reduction suggests that long-term radon radiation damage may decrease immune system function. Immune-related diseases can affect any organ or system, including the lungs.[21]

At the same time, we found that the cell cycle of lymphocytes also changed. The prolongation of the G_0G_1 phase is an important indicator of cell repair after radiation damage; the shortening of S phase suggests a decrease in cell division. This result is consistent with the fact that α-particle irradiation inhibits DNA synthesis and subsequently leads to cell cycle arrest. The decrease in LYM is consistent with previous studies that showed a positive correlation between LYM and the duration of exposure to acute external radiation.[22,23] However, whether LYM decreases due to cell necrosis, apoptosis, or migration to other organs and tissues remains to be further studied.

In our study, cyclins and CDKs increased in the underground group compared with the control group, suggesting that the lymphocytes were damaged. This is similar to previous studies that showed that overexpression of cell cycle regulatory proteins is closely related to human diseases including cancer. For example, Cyclin D and Cyclin E are overexpressed in the early stage of gastric carcinoma,[24] cell cycle defects associated with tumors are often mediated by alterations in CDK activity, and CDK dysregulation induces genomic and chromosomal instability.[25] There is also research on blocking CDK4/6 for the treatment of acute gastrointestinal toxicity due to radiation therapy to observe the effects of different radiation therapy regimens.[26]

The relative expression of 4 miRNAs, miR-19a, miR-30e, miR-335, and miR-451a, decreased in the underground group miners compared with the control group. MiR-19a in peripheral blood leukocytes is an effective biomarker for early detection of silicosis[27]; miR-30 is downregulated in non-small cell lung cancer[28] and human primary squamous cell lung carcinoma[29]; miR-335 inhibits small cell lung cancer bone metastases[30]; and miR-451 is significantly downregulated in docetaxel-resistant

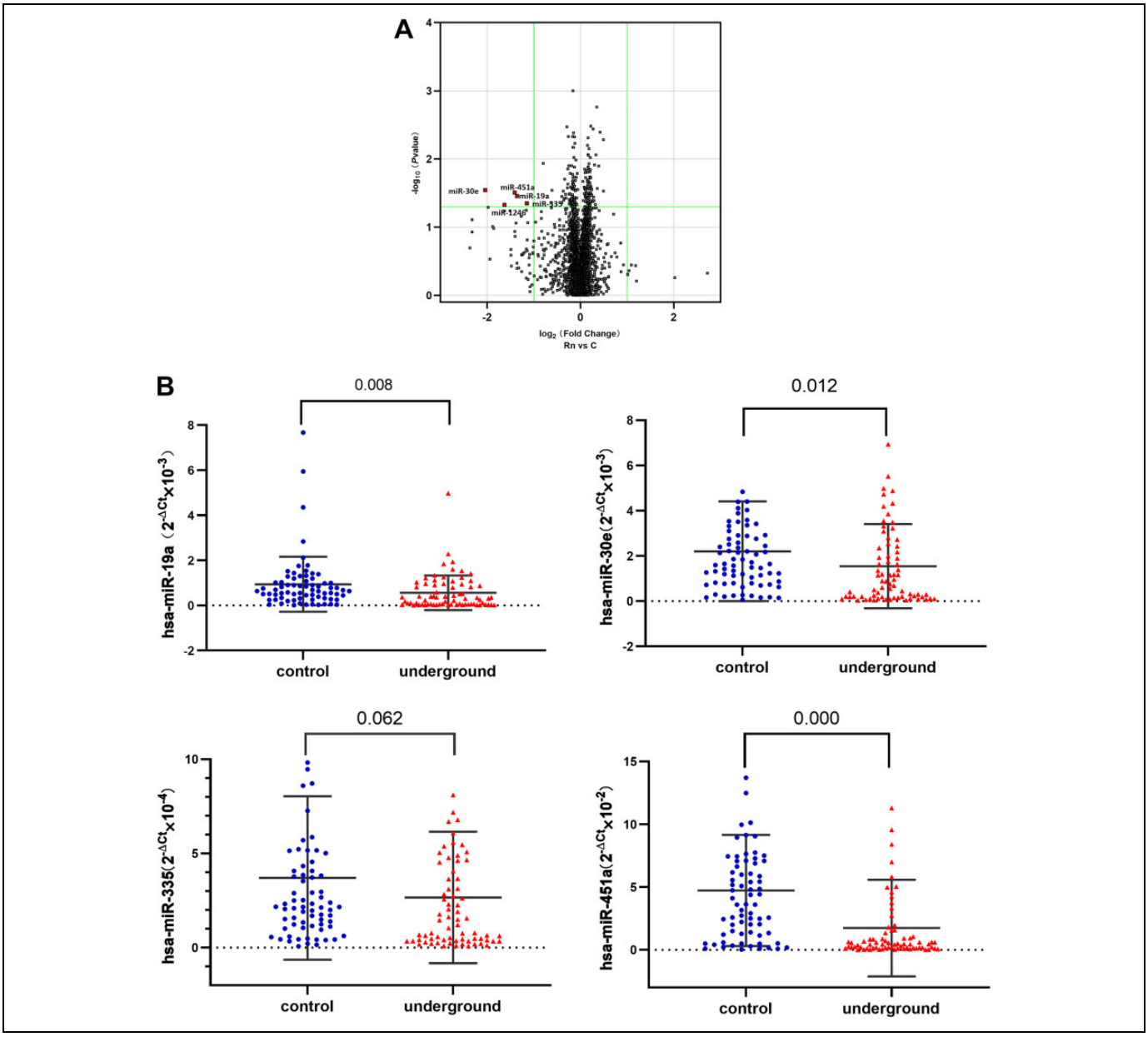

Figure 3. MicroRNA (miRNA) microassay analysis and miRNA detection using real-time polymerase chain reaction (PCR). A, Volcano plot of miRNA expression based on miRNA microarray screening and comparison between group Rn (>40 years old) and group C (<40 years old). The odds ratio is plotted on the x-axis and the negative log10 (*P* value) is plotted on the y-axis. B, Comparison of miR-19a, miR-30e, miR-335, and miR-451a detected using real-time PCR between the underground and control groups (n = 72 per group). *P* values were calculated using the Wilcoxon test.

lung adenocarcinoma cells, and overexpression of miR-451 inhibited invasion and metastasis of docetaxel-resistant lung adenocarcinoma cells both in vitro and in vivo.[31] Nevertheless, our results are inconsistent with those of miRNA screening in radon-exposed mice[32]; the results may be related to the differences between species, cell lines, and the complexity of the radon exposure environment. Previous studies have shown little difference in miRNA expression between plasma and lymphocytes in the same population,[33,34] and our Pearson correlation analysis of miRNAs (in plasma) and target proteins (in lymphocytes) showed negative correlations, which indicates a potentially convenient method for clinical detection.

We also analyzed the effect of smoking on the potential biomarkers (LYM and NE), and we found that smoking had a relatively small effect on the potential biomarkers in both the underground and control groups. Although there was a relatively higher expression in underground miners in the nonsmoking and light smoking subgroups, the differences were not significant. Our data demonstrated that if smoking and radon act simultaneously, the difference between groups is

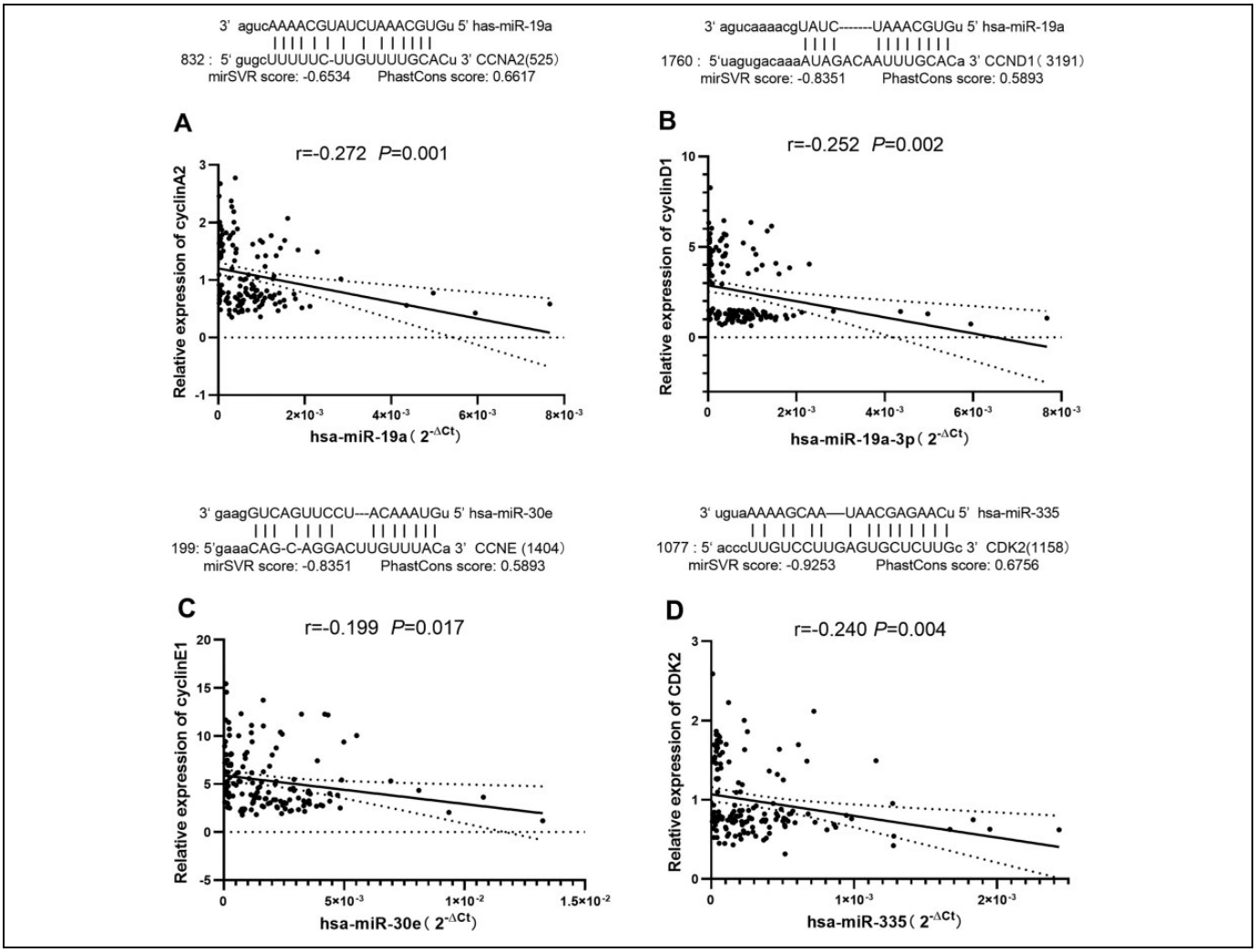

Figure 4. Correlations between microRNAs (miRNAs) and proteins. There were significant negative correlations between the relative expression of (A) Cyclin A2 protein and miR-19a, (B) Cyclin D1 protein and miR-19a, (C) Cyclin E1 protein and miR-30e, and (D) cyclin-dependent kinase (CDK)-2 protein and miR-335 (n = 144). Pearson correlation coefficient and *P* value were calculated.

significant. This finding confirms the conclusion of another study showing that the risk associated with radon exposure is greater than that associated with tobacco in miners.[35]

The limitation of this study is that we focused on the change in LYM in the peripheral blood (and the interrelations between various potential biomarkers) under radon exposure, but the change in NE under radon exposure was also significantly different. Additionally, no predicted direct target protein of miR-451a related to the cell cycle was found in the plasma analysis. The downregulation of miR-451a may affect the cell cycle or certain signaling pathways, and this needs further study.

Conclusions

We are concerned about the health of the occupational population exposed to radon. The changes in potential biomarkers in peripheral blood may be related to cumulative radon exposure. Our results indicate that LYM, NE, CDK2, CDK4, CDK6, Cyclin A2, Cyclin D1, Cyclin E1, miR-19a, miR-30e, miR-335, and miR-451a are potential biomarkers of radon radiation damage. Long-term follow-up is needed to gather and analyze data on radiation-induced diseases.

Acknowledgments

The authors thank every researcher in this study.

Declaration of Conflicting Interests

The author(s) declared no potential conflicts of interest concerning the research, authorship, and/or publication of this article.

Funding

The author(s) received no financial support for the research, authorship, and/or publication of this article.

ORCID iDs

Lu Sun https://orcid.org/0000-0003-2000-7771
Chunnan Piao https://orcid.org/0000-0002-4349-9564

References

1. US Environmental Protection Agency. A citizen's guide to radon. 2010. www.epa.gov. Accessed January 29, 2012.
2. International Programme on Chemical Safety (IPCS). *Environmental Health Criteria 211. Health Effects of Interactions Between Tobacco Use and Exposure to Other Agents*. Geneva, Switzerland: WHO; 1999.
3. National Research Council, Committee on Health Risks of Exposure to Radon. *Health Effects of Exposure to Radon (BEIR VI)*. Washington, DC: National Academy Press; 1999.
4. Kreuzer M, Sobotzki C, Schnelzer M, Fenske N. Factors modifying the radon-related lung cancer risk at low exposures and exposure rates among German uranium miners. *Radiat Res*. 2018; 189(2):165-176.
5. Rage E, Caer-Lorho S, Drubay D, Ancelet S, Laroche P, Laurier D. Mortality analyses in the updated French cohort of uranium miners (1946-2007). *Int Arch Occup Environ Health*. 2015;88(6): 717-730.
6. Krewski D, Lubin JH, Zielinski JM, et al. Residential radon and risk of lung cancer a combined analysis of 7 North American case–control studies. *Epidemiology*. 2005;16(2):137-145.
7. Occupational intakes of radionuclides: part 3. ICRP Publication 137. Ann. ICRP 46(3/4). France: ICRP; 2017.
8. Sherry CJ, Roberts JM. Living with or without cyclins and cyclin dependent kinases. *Genes Dev*. 2004;18(22):2699-2711.
9. Sherry CJ, Roberts JM. CDK inhibitors: positive and negative regulators of G1-phase progression. *Genes Dev*. 1999;13(12): 1501-1512.
10. Liang J, Liu X, Xue H, Qiu B, Wei B, Sun K. MicroRNA-103a inhibits gastric cancer cell proliferation, migration and invasion by targeting c-Myb. *Cell Prolif*. 2015;48(1):78-85.
11. Karp X, Ambros V. Developmental biology. Encountering microRNAs in cell fate signaling. *Science*. 2005;310(5752):1288-1289.
12. Cheng AM, Byrom MW, Shelton J, Ford LP. Antisense inhibition of human miRNAs and indications for an involvement of miRNA in cell growth and apoptosis. *Nucleic Acids Res*. 2005;33(4): 1290-1297.
13. Meng W, Efstathiou J, Singh R, et al. MicroRNA biomarkers for patients with muscle-invasive bladder cancer undergoing selective bladder-sparing trimodality treatment. *Int J Radiat Oncol Biol Phys*. 2019;104(1):197-206.
14. Sun YL, Hawkins PG, Bi N, et al. Serum microRNA signature predicts response to high-dose radiation therapy in locally advanced non-small cell lung cancer. *Int J Radiat Oncol Biol Phys*. 2018;100(1):107-114.
15. Verma AM, Patel M, Aslam MI, et al. Circulating plasma microRNAs as a screening method for detection of colorectal adenomas. *Lancet*. 2015;385(suppl 1):S100.
16. Frampton AE, Castellano L, Colombo T, et al. Integrated molecular analysis to investigate the role of microRNAs in pancreatic tumour growth and progression. *Lancet*. 2015;385(suppl 1):S37.
17. Chen ZH, Wang DP, Gu C, et al. Down-regulation of let-7 microRNA increased K-ras expressing in lung damage induced by radon. *Environ Toxicol Pharmacol*. 2015;40(2):541-548.
18. Li BY, Sun J, Wei H, et al. Radon-induced reduced apoptosis in human bronchial epithelial cells with knockdown of mitochondria DNA. *J Toxicol Environ Health A*. 2012;75(18):1111-1119.
19. Chen WQ, Zheng RS, Baade PD, et al. Cancer statistics in China, 2015. *CA Cancer J Clin*. 2016;66(2):115-132.
20. Livak KJ, Schmittgen TD. Analysis of relative gene expression data using real-time quantitative PCR and the 2(−delta delta C(T)) methods. *Methods*. 2001;25(4):402-408.
21. Postow MA, Sidlow R, Hellmann MD. Immune-related adverse events associated with immune checkpoint blockade. *N Engl J Med*. 2018;378(2):158-168.
22. Goan RE, Holloway EC, Berger ME, Ricks RC. Early dose assessment in criticality accidents. *Health Phys*. 2001;81(4): 446-449.
23. Azizova TV, Osovets SV, Day RD, et al. Predictability of acute radiation injury severity. *Health Phys*. 2008;94(3):255-263.
24. Kumari S, Puneet, Prasad SB, et al. Cyclin D1 and cyclin E2 are differentially expressed in gastric cancer. *Med Oncol*. 2016;33(5): 40.
25. Malumbres M, Barbacid M.Cell cycle, CDKs and cancer: a changing paradigm. *Nat Rev Cancer*. 2009;9(3):153-166.
26. Lee CL, Oh P, Xu ES, et al. Blocking cyclin-dependent kinase 4/6 during single dose versus fractionated radiation therapy leads to opposite effects on acute gastrointestinal toxicity in mice. *Int J Radiat Oncol Biol Phys*. 2018;102(5):1569-1576.
27. Yang Z, Li Q, Yao SQ, et al. Down-regulation of miR-19a as a biomarker for early detection of silicosis. *Anat Rec (Hoboken)* 2016;299(9):1300-1307.
28. Markou A, Sourvinous I, Vorkas PA, Yousef GM, Lianidou E. Clinical evaluation of microRNA expression profiling in non small cell lung cancer. *Lung Cancer*. 2013;81(3):388-396.
29. Gao W, Shen H, Liu L, Xu J, Xu J, Shu Y. MiR-21 overexpression in human primary squamous cell lung carcinoma is associated with poor patient prognosis. *J Cancer Res Clin Oncol*. 2011; 137(4):557-566.
30. Gong M, Ma JR, Guillemette R, et al. Mir-335 inhibits small cell lung cancer bone metastases via IGF-IR and RANKL pathways. *Mol Cancer Res*. 2014;12(1):101-110.
31. Chen D, Huang J, Zhang K, et al. MicroRNA-451 induces epithelial–mesenchymal transition in docetaxel-resistant lung adenocarcinoma cells by targeting proto-oncogene c-Myc. *Eur J Cancer*. 2014;50(17):3050-3067.
32. Cui FM, Li JX, Chen Q, et al. Radon-induced alterations in microRNA expression profiles in transformed BEAS2B cells. *J Toxicol Environ Health A*. 2013;76(2):107-119.
33. Liu CX, Li XL, Pan Y, et al. Expression of miRNAs in peripheral blood lymphocytes of the residents around hot springs with radon. *Carcinog Teratog Mutagen*. 2015;27:446-449.
34. Liu CX, Tian M, Pan Y, Gao G, Liu J. Expression of miRNAs in peripheral blood plasma of the residents surrounding hot springs with radon. *Chin J Radiol Med Prot*. 2015;35(3):187-190.
35. Qiao YL, Taylor PR, Yao SH, et al. Relation of radon exposure and tobacco use to lung cancer among tin miners in Yunnan Province, China. *Am J Ind Med*. 1989;16(5):511-521.